IOP PUBLISHING EUROPEAN JOURNAL OF PHYSICS

Eur. J. Phys. **28** (2007) 845–857 doi:10.1088/0143-0807/28/5/008

Rotational stability—an amusing physical paradox

Carlos M Sendra[1], Fabricio Della Picca[1] and Salvador Gil[1,2]

[1] Departamento de Física, J J Giambiagi, Universidad de Buenos Aires, Argentina
[2] Escuela de Ciencia y Tecnología, Universidad Nacional de San Martín, Campus Miguelete, M de Irigoyen 3100, San Martín (1650), Buenos Aires, Argentina

E-mail: sgil@unsam.edu.ar

Received 1 May 2007, in final form 7 June 2007
Published 12 July 2007
Online at stacks.iop.org/EJP/28/845

Abstract

Here we present a simple and amusing device that demonstrates some surprising results of the dynamics of the rotation of a symmetrical rigid body. This system allows for a qualitative demonstration or a quantitative study of the rotation stability of a symmetric top. A simple and inexpensive technique is proposed to carry out quantitative measurements to explore the theoretical predictions of the model presented to explain the motion of the system. Our results agree very well with the expectations of the theoretical model.

(Some figures in this article are in colour only in the electronic version)

1. Introduction

It is rewarding and instructive to share with friends and the public in general the fun and excitement that we physicists often obtain from exploring the ways in which nature behaves. Here we present a simple device that can be used to entertain friends at a party, while illustrating the kind of problem a physicist enjoys working on. It can also be used in a regular laboratory course to carry out quantitative measurements to explore the physics of the rotational stability of a rigid body. The experiment consists of a rod the size of a pen or a ring attached to a flexible wire or a fishing line of about 30 cm as illustrated in figure 1. At rest the rod or the ring (symmetric top) hangs, as expected, with its centre of mass at its lowest position. If we start spinning the wire with our fingers, the rod or the ring rotates with their centre of mass in the same position, but if we increase the rotation frequency above a critical value, the symmetric top begins to raise its centre of mass approaching a horizontal position as the frequency increases. The rising of the centre of mass is at first sight surprising and contrary to our intuition. If we naively attempt to calculate the potential and kinetic energy of the bar at a given inclination, both terms increase monotonically with the elevation of the centre of mass

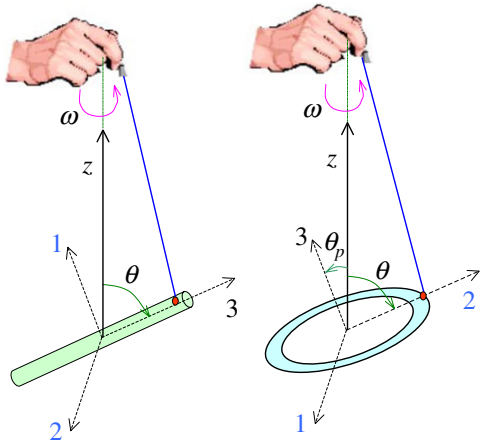

Figure 1. Symmetric top rotating along the z axis. Left: the position adopted by a bar when it is being spun through the wire with our fingers. Right: the figure shows the corresponding equilibrium position of the ring when it is rotating. Axis 3 represents the symmetry axis, whereas axes 1 and 2 are the other principal directions of the body.

independent of the angular frequency of rotation. Therefore, the observed effect appears to be paradoxical.

The physics of the symmetrical top has important applications in several areas of physics, such as classical mechanics, molecular, nuclear physics and astrophysics. Therefore its understanding and inclusion in introductory and intermediate level courses is well justified and the development of new experiments to explore its physics is also welcome. The physics of the free rotating top is treated in most introductory and intermediate level texts on mechanics [1–4]. There are also a number of very instructive and amusing demonstrations of the motion of symmetric and asymmetric tops [5–8] among which the gyroscope is a classic example. Nonetheless, the literature of experiments on this subject that allows for precise quantitative measurements, which can be contrasted with the corresponding theory or models, is very scarce.

In this work we develop a simple model to understand this behaviour qualitatively. Then we develop a more refined model that can be directly compared with the experimental results. The models can be readily tested using the results of the experiment. We analyse the case of a bar and a ring.

2. Theoretical considerations

We begin examining the case of the rotating rod, whose length is h and mass is m, that hangs from a very long wire of length L ($\gg h$). This system is illustrated schematically in figure 2. The spinning angular frequency is ω along the z axis (in the space-fixed or inertial frame of reference).

The behaviour of the bar becomes clear if we visualize our system from a body-fixed frame of reference. In this frame, which rotates with frequency ω around the z axis, there are two torques in opposite directions. The torque due to the string tension, τ_w, tends to restore the rod to the vertical direction and the torque due to the centrifugal force [1, 2], τ_c, tends to

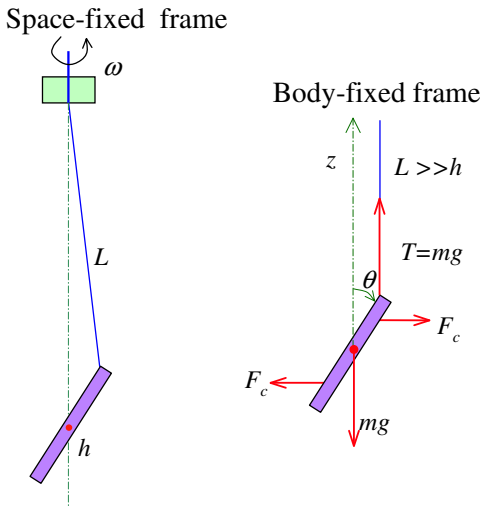

Figure 2. Schematic representation of a rod, of length h, that is being spun at an angular frequency ω along the z axis by a long wire of length L. Left: the bar is shown in the space-fixed frame of reference. Right: the bar is shown in the body-fixed frame (rotating frame) of reference. Here we assume that $L \gg h$. Therefore, the string is almost parallel to the vertical direction (naïve model).

bring the rod to a horizontal position. We take the centre of mass of the rod as a reference point for calculating the torques. In equilibrium these two torques are equal, therefore

$$\tau_w = m.g.\frac{h}{2} \cdot \sin\theta = \tau_c = m \cdot \omega^2 \frac{h^2}{12} \cdot \sin\theta \cdot \cos\theta. \tag{1}$$

The details of the calculation of the centrifugal torque are presented in appendix A. From equation (1) it follows that the equilibrium position of the rod is determined by

$$\cos\theta = \frac{6g}{h\omega^2} = \left(\frac{\omega_{c0}}{\omega}\right)^2, \tag{2}$$

with

$$\omega_{c0} = \sqrt{\frac{6g}{h}}. \tag{3}$$

In order to obtain a solution of equation (1) different to $\theta = 0$ the condition $\omega \geqslant \omega_{c0}$ must be satisfied. Consequently, we expect that at low rotational frequencies, $\omega < \omega_{c0}$, the rod will rotate in the vertical position ($\theta = 0$), for $\omega > \omega_{c0}$, the angle θ will increase as ω increases, in accordance with equation (2). We will call the model just discussed the naïve model. A more general discussion of this problem is presented in appendices A and B, where the case of a finite length of wire, and other geometries for the symmetrical top, are also considered. The derivation presented in appendix A should be accessible to beginner students, whereas the model discussed in appendix B requires some knowledge of intermediate analytical mechanics [1–4].

3. The experiment

The experimental arrangement we used is shown in figure 3. It consisted of a variable speed dc motor (with mechanical reduction) powered by a variable dc voltage source, that regulates the

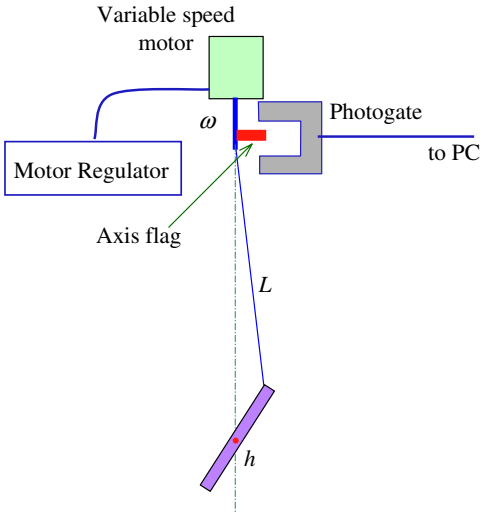

Figure 3. Schematic representation of a rod, of length h, that is being spun at an angular frequency ω by a variable speed motor.

speed of the motor. We taped a plastic tube to the axis of the motor (axis flag) to interrupt the beam of light of a photogate on every rotation. The photogate, connected to a computer, was used to monitor the speed of the motor and measure its rotational frequency ω. As symmetrical tops we used aluminium tubes of about 9 mm in an external diameter with different lengths h. We drilled a small hole close to one of their extremes to attach a thin wire of length L that was connected to the axis of the motor. We used a general purpose PVC insulated electronic hook-up wire gauge 24 and about 35 cm in length. Its mass was less than 0.5% of the mass of the rod and was neglected in our analysis. We also used metal rings of diameters between 5 and 10 cm.

A WebCam (Genius GE11) was used to obtain the digital photographs of the tops, once they reached an equilibrium position. A plumb line was placed in the background to determine the angle θ of the bar or ring. An advantage of many inexpensive WebCams, such as the one used here, is that as the illumination gets dimmer the shutter speed of the camera is reduced. Therefore, by regulating the illumination it is possible to obtain a photograph of the bar or ring that averages over several positions of the top as shown in figure 4, where we clearly see the orientation of the rod. These digital pictures allow us to obtain the orientation angle θ with a few degrees of uncertainty for every frequency of the motor. Naturally, the same effect could be obtained using a digital camera with shutter speed regulation. Another alternative that can be used for measuring the orientation angle θ is to use the digital camera in video mode. The procedure would involve recording a few revolutions of the top, and then examining the video frame by frame to select the one where the wire and the bar are in the plane of the picture. Then the picture is used to proceed as suggested in figure 4.

4. Results and discussion

In figure 5, we present the experimental results (symbols) obtained for a hollow aluminium bar of length $h = 25.5$ cm and an external diameter $d = 0.95$ cm, attached to a thin wire of $L = 33.4$ cm to a point on the bar at $\delta = 0.8$ cm from one of its extremes. In the same figure

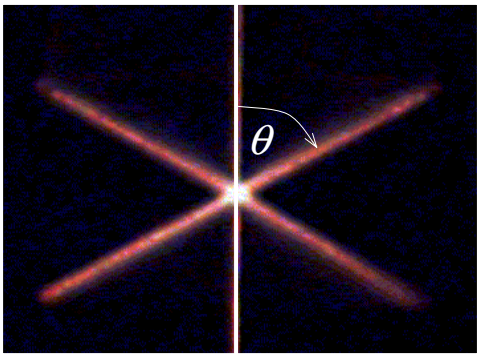

Figure 4. Photograph of the rotating bar. A slow shutter speed was used such that each shot averaged over several orientations of the bar. In the background the image of the plumb line is shown that was used to define the vertical direction. This type of digital picture allowed us to obtain the rotational equilibrium angle θ with an uncertainty of about 2° for each rotational frequency.

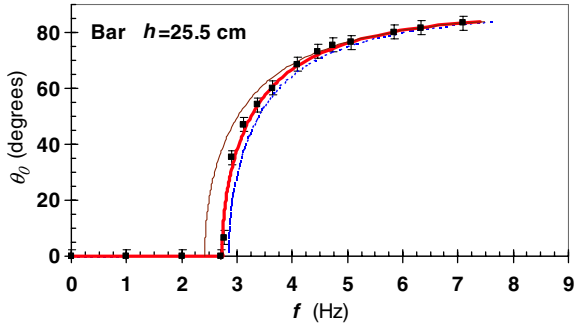

Figure 5. The symbols represent the experimental results for a bar ($h = 25.5$ cm). The dotted line corresponds to the prediction of the naïve model given by equation (2). The dashed line corresponds to the expectation of the model (no. 2) discussed in appendix A where the finite length of the wire is included. The heavy line is the prediction of the model (no. 3) discussed in appendix B where both the finite length of the wire and the distance δ of the point of connection to the wire are also considered. In this case, $L = 33.4$ cm and $\delta = 0.8$ cm.

we also show the theoretical expectation of the naïve model equation (2). The models that include the finite length of the wire and the distance δ of the point of attachment to the extreme of the bar are also depicted in the same figure.

It is clear that for an adequate description of the experimental data model no. 3 that includes both the finite length of the wire and the distance δ is necessary. This model is developed in appendix B. In figure 6, we show the experimental results for another bar of a different length and for a ring. In this figure we have also included the prediction of model no. 3. Out of all the cases analysed in this work model no. 3 gives a very good description of the observed results. It is interesting to note that due to the effect of the centrifugal force, at high rotational frequencies, the driven symmetrical top tends to rotate about the axis of the largest moment of inertia, independently of whether it is a symmetry axis or not.

In summary, we have devised a simple and inexpensive experiment that can be implemented in an introductory or intermediate laboratory class on classical mechanics. We also developed a realistic model that adequately reproduces the experimentally observed

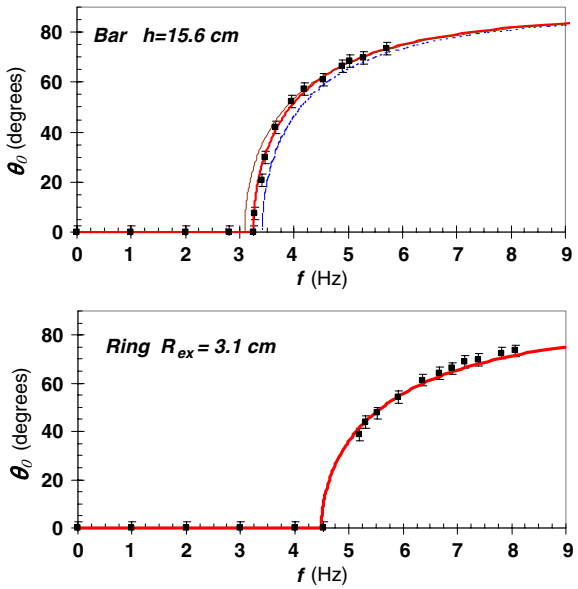

Figure 6. Experimental results (symbols) for a bar and a ring. The heavy continuous lines are the expectation of the theoretical model (no. 3) presented in appendix B. The other lines in the case of the bar are the prediction of the naïve model (dotted) and model no. 2 (dashed).

equilibrium orientations of a spinning symmetrical top that can be used to study the rotational stability of a rotating top. Our results are complementary to the analysis of supercritical bifurcation carried out, with a different approach, for the case of the ring using a similar experimental setup [9].

Acknowledgments

We would like to express our acknowledgment to other students who have explored the physics of our systems with different experimental techniques: V Bazterra, A Camjayi, M Mansilla, A Solernó and J Tiffenberg. We express our sincere gratitude to Professor F Scarlassara for an illuminating discussion and a very contributory revision of this article. We are also grateful to Dr A Schwint for careful reading of the manuscript.

Appendix A. Improved model of a rotating rod—model no. 2

Consider a rod forming an angle θ with the vertical. In the body-fixed frame, there is a centrifugal force that tends to bring the rod to a horizontal position and the string tension and weight that tend to restore the rod to the vertical position. The system is illustrated in figure 7. Throughout all our analysis we will assume that the string or wire is longer than the bar, i.e. $L > h$. The equilibrium of the vertical and horizontal forces implies that

$$T\cos\beta = mg \qquad \text{and} \qquad T\sin\beta = F_c^{(cm)} = m\omega^2\varepsilon\sin\theta, \tag{A.1}$$

where T is the string tension and $F_c^{(cm)}$ is the centrifugal force acting on the centre of mass that is revolving around the vertical that passes through the point of suspension, the net centrifugal force. Here ε is the distance of the centre of mass of the rod to the point O (figure 7) where

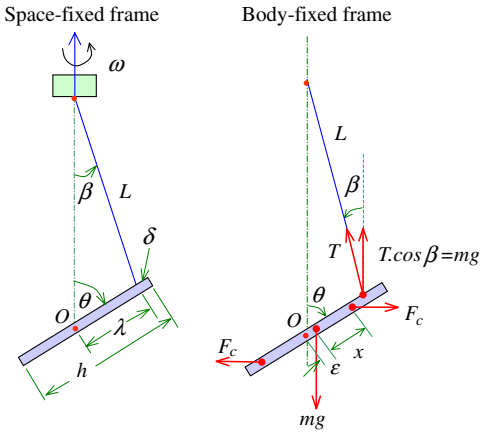

Figure 7. Schematic representation of a rod, of length h, that is being spun at an angular frequency ω by a string of length L. Left: the system is in the fixed or inertial frame of reference. Right: the system is in the body frame of reference (rotating). The point O on the rod is the intersection of the axis of the rod with the vertical that passes through the point of suspension of the string, λ is the distance from point O to the point of attachment of the wire.

the axis of the rod intersects the vertical that goes through the point of suspension. From the geometry of our system we have that

$$\lambda \cdot \sin\theta = L \sin\beta, \tag{A.2}$$

where λ is the distance from O to the point of attachment of the wire, therefore

$$\tan\beta = \frac{\lambda}{L} \cdot \frac{\sin\theta}{\sqrt{1-(\lambda/L)^2\sin^2\theta}}. \tag{A.3}$$

From the geometry (figure 7) we have that $\lambda = h/2 - \delta + \varepsilon$, where δ is the distance from the point attachment of the wire to the extreme of the bar. From (A.1) it follows that

$$\varepsilon = \frac{g}{\omega^2}\frac{\lambda}{L} \cdot \frac{1}{\sqrt{1-(\lambda/L)^2\sin^2\theta}}. \tag{A.4}$$

Note that $\varepsilon > 0$ if L is finite, since ε depends on the ratio $\lambda/L \approx h/2L$, $\varepsilon \to 0$ for $L \gg h$. This expression provides an implicit dependence of ε with θ and ω, since λ also depends on ε. The values of ε and λ can be calculated recursively as we indicate below.

All torques will be calculated using the point O as a reference. The torque due to the centrifugal force on an infinitesimal element of rod dx at a distance x from the centre of mass is

$$\mathrm{d}\tau_c = (x+\varepsilon)\cdot\cos\theta\cdot\mathrm{d}F_c = (x+\varepsilon)^2\cdot\cos\theta\cdot\mathrm{d}m\cdot\omega^2\cdot\sin\theta. \tag{A.5}$$

Here ω is the angular velocity of the rod and $\mathrm{d}m = (m/h)\cdot\mathrm{d}x$ is the mass of the infinitesimal element of the rod. Since $\lambda \approx h/2$, the total centrifugal torque will be

$$\tau_c \approx \frac{m}{h}\cos\theta\cdot\sin\theta\cdot\omega^2\cdot\int_{-h/2}^{h/2}(x+\varepsilon)^2\cdot\mathrm{d}x = \frac{m}{12}h^2\omega^2\cos\theta\sin\theta\cdot[1+12\varepsilon^2/h^2]. \tag{A.6}$$

The torque due to the weight of the rod and the string tension is

$$\tau_w = mg\lambda\cdot\sin\theta + mg\cdot\frac{\sin\beta}{\cos\beta}\lambda\cos\theta - mg\varepsilon\sin\theta, \tag{A.7}$$

or

$$\tau_w = mg(\lambda - \varepsilon) \cdot \sin\theta \cdot \left[1 + \frac{\lambda}{(\lambda - \varepsilon)} \frac{\lambda}{L} \frac{\cos\theta}{\sqrt{1 - (\lambda/L)^2 \sin^2\theta}}\right]. \tag{A.8}$$

In equilibrium $\tau_w - \tau_c$, therefore

$$\omega^2 = \frac{6g}{h} \cdot \left[\frac{1}{\cos\theta} + \frac{\lambda}{(\lambda - \varepsilon)} \frac{\lambda}{L} \cdot \frac{1}{\sqrt{1 - (\lambda/L)^2 \sin^2\theta}}\right] \cdot \frac{2(\lambda - \varepsilon)/h}{(1 + 12\varepsilon^2/h^2)}, \qquad \text{for} \quad \omega \geqslant \omega_{\text{crit}}. \tag{A.9}$$

This relation describes the connection between θ and ω. Note that this is an implicit equation between these variables. Its solution can be found recursively. First, based on the connection between θ and ω given by the naïve model, we can calculate $\varepsilon(\theta, \omega)$ using equation (A.4). This value of ε then allows us to calculate λ. Using equation (A.9) we obtain improved values of θ and ω. This process can be repeated to the desired precision. In our experience, two or three iterations are sufficient to determine θ and ω with 1–2% of uncertainty. The critical value of ω_{crit} is obtained from (A.9) for $\theta = 0$, i.e.,

$$\omega_{\text{crit}}^2 = \frac{6g}{h} \cdot \left[1 + \frac{h}{2L} \frac{1}{\left(1 - \frac{2\delta}{h}\right)} \left(1 - \frac{2\delta}{h} + \frac{2\varepsilon_c}{h}\right)^2\right] \cdot \frac{\left(1 - \frac{2\delta}{h}\right)}{\left(1 + \frac{12\varepsilon_c^2}{h^2}\right)}, \tag{A.10}$$

since $\lambda - \varepsilon = h/2 - \delta$, to first order in δ/h and ε/h, this last expression becomes

$$\begin{aligned} \omega_{\text{crit}}^2 &\approx \frac{6g}{h} \cdot \left[1 - \frac{2\delta}{h} + \frac{h}{2L}\left(1 - \frac{4\delta}{h} + \frac{4\varepsilon_c}{h}\right)\right] \\ &\approx \omega_{c0}^2 \cdot \left[1 + \frac{h}{2L} - \frac{2\delta}{h} - \frac{2\delta}{L} + \frac{2\varepsilon_c}{L}\right], \end{aligned} \tag{A.11}$$

where $\varepsilon_c = \varepsilon(\omega_{\text{crit}}, \theta = 0) \approx \left(g/\omega_{c0}^2\right)(\lambda/L)$ is the value of ε at the critical frequency. Since in general ε_c and δ are small compared with h or L, see figure 9, we neglected the second-order terms in (ε/h). Expression (A.11) can be further approximated for the case of $\delta \ll h$ and $\varepsilon \ll h < L$ as

$$\omega_{\text{crit}}^2 \approx \omega_{c0}^2 \cdot \left[1 + \frac{h}{2L}\right]. \tag{A.12}$$

Consequently, the effect of the finite length of the wire is to move ω_{crit} to the right of the value predicted by the naïve model equation (3). For $L \gg h$, the expressions (A.9) and (A.11) are reduced to equations (2) and (3) respectively.

The z coordinate of the centre of mass, relative to its lowest position is

$$z_{\text{CM}} = L + (\lambda - \varepsilon) - \sqrt{L^2 - \lambda^2 \cdot \sin^2\theta} - (\lambda - \varepsilon) \cdot \cos\theta, \tag{A.13}$$

and

$$\frac{\mathrm{d}z_{\text{CM}}}{\mathrm{d}t} = (\lambda - \varepsilon)\sin\theta \cdot \left(1 + \left(\frac{\lambda}{\lambda - \varepsilon}\right) \cdot \frac{\lambda\cos\theta}{\sqrt{L^2 - \lambda^2 \cdot \sin^2\theta}}\right) \cdot \dot{\theta}, \tag{A.14}$$

where $(\lambda - \varepsilon)$ is the distance of the centre of mass to the hanging point of the bar.

Appendix B. Effective potential—model no. 3

For the analysis of the rotational stability of a symmetrical top, subject to a movable constraint (wire) in a more general manner, it is useful to obtain the effective potential. To this purpose we use the Lagrangian formulation of the problem [1–4]. Let us denote the principal axes of

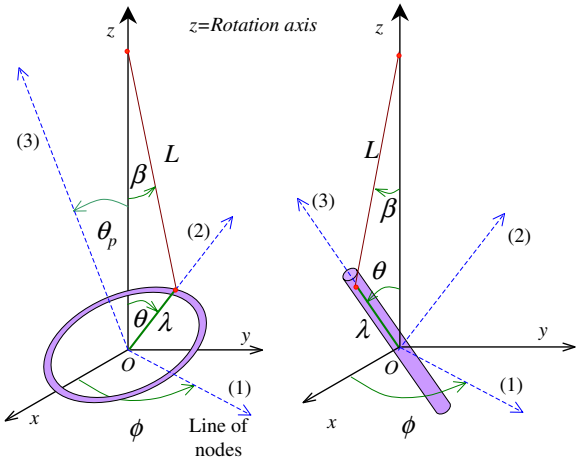

Figure 8. Rotating symmetrical tops. We assume that $\omega = \dot{\phi}$ and $\dot{\psi} = 0$, since there is no rotation around axis 3. λ is the distance from point O to the hanging point. Left: illustrates the case of a ring-like top. Right: corresponds to the rod-like top.

inertia of the top by 1, 2 and 3, axis 3 being the symmetry axis. Due to this symmetry the moments of inertia along axes 1 and 2 are equal, i.e. $I_{12} = I_1 = I_2 \neq I_3$. The z axis (inertial frame) is chosen to be in the vertical direction. We take $z = 0$ to coincide with the lowest position of the centre of mass of the top.

The Lagrangian of this system is

$$L = T_{\text{tras}} + T_{\text{rot}} + T_{\text{rot}}^{(\text{cm})} - V_{\text{grav}}, \tag{B.1}$$

where T_{tras} is the translational kinetic energy associated with the raising or lowering of the centre of mass of the top. According to (A.10) we have

$$T_{\text{tras}} = \frac{1}{2}m \cdot \left(\frac{\mathrm{d}z_{CM}}{\mathrm{d}t}\right)^2 = \frac{1}{2}m\left((\lambda - \varepsilon)\sin\theta \cdot \left(1 + \frac{\lambda^2}{(\lambda - \varepsilon)}\frac{\cos\theta}{\sqrt{L^2 - \lambda^2 \cdot \sin^2\theta}}\right) \cdot \dot{\theta}\right)^2, \tag{B.2}$$

where $(\lambda - \varepsilon)$ is the distance from the centre of mass to the hanging point of the top. In the case of the bar, $(\lambda - \varepsilon) \approx h/2$ and for a ring $(\lambda - \varepsilon) \approx$ radius. The term $T_{\text{rot}}^{(\text{cm})}$ indicates the kinetic rotational energy of the centre of mass, i.e.,

$$T_{\text{rot}}^{(\text{cm})} = \frac{1}{2}m\omega^2\varepsilon^2\sin^2\theta = \frac{1}{2}m\frac{g^2}{\omega^2}\left(\frac{\lambda}{L}\right)^2\frac{\sin^2\theta}{1 - (\lambda/L)^2\sin^2\theta}. \tag{B.3}$$

The rotational kinetic energy, T_{rot}, written in terms of the Euler angles [1–4], for a symmetrical top is

$$T_{\text{rot}} = \frac{1}{2}\sum_i I_i\omega_i^2 = \frac{1}{2}[I_{12}(\dot{\theta}^2 + \dot{\phi}^2\sin^2\theta) + I_3(\dot{\psi} + \dot{\phi}\cos\theta)^2], \tag{B.4}$$

where θ, ϕ and ψ are the Euler angles that are used in our problem as generalized coordinates as indicated in figure 8. As usual, ψ describes the rotation of the top around axis 3 [1, 2]. In our case there is no rotation around this axis, since the wire does not twist, we have that $\psi =$ constant and $\dot{\psi} = 0$. The constraint imposed by the rotating wire implies that $\dot{\phi} = \omega$. Therefore, according to our model θ becomes the only degree of freedom for our system and

we use it as the generalized coordinate to describe its state. Expression (B.4) is different for the cases of a ring-like and the rod-like tops as illustrated in figure 8. In the case of a rod-like top we have

$$T_{\text{rot}} = \tfrac{1}{2}[I_{12}(\dot{\theta}^2 + \omega^2 \sin^2\theta) + I_3\omega^2\cos^2\theta]. \tag{B.5}$$

In the case of a ring-like top we have

$$T_{\text{rot}} = \tfrac{1}{2}\big[I_{12}(\dot{\theta}_p^2 + \omega^2 \sin^2\theta_p) + I_3\omega^2\cos^2\theta_p\big], \tag{B.6}$$

with $\theta_p = \pi/2 - \theta$ and $\dot{\theta}_p = -\dot{\theta}$. If we introduce a new variable, χ so that

$$\chi = \begin{cases} \pi/2 & \text{for the case of the ring-like top} \\ 0 & \text{for the case of the rod-like top.} \end{cases} \tag{B.7}$$

Then expressions (B.5) and (B.6) can be cast in a single convenient form

$$T_{\text{rot}} = \tfrac{1}{2}[I_{12}(\dot{\theta}^2 + \omega^2 \sin^2(\chi - \theta)) + I_3\omega^2\cos^2(\chi - \theta)], \tag{B.8}$$

For the gravitational potential energy according to equation (A.13) we have

$$V_{\text{grav}} = mg \cdot z = mg \cdot [L + (\lambda - \varepsilon)(1 - \cos\theta) - \sqrt{L^2 - \lambda^2 \cdot \sin^2\theta}]. \tag{B.9}$$

Consequently, the Lagrangian of our system is

$$\begin{aligned} L = {} & \frac{1}{2}m(\lambda-\varepsilon)^2\sin^2\theta \cdot \left(1 + \frac{\lambda^2}{(\lambda-\varepsilon)}\frac{\cos\theta}{\sqrt{L^2 - \lambda^2\cdot\sin^2\theta}}\right)^2 \cdot \dot{\theta}^2 \\ & + \frac{1}{2}[I_{12}(\dot{\theta}^2 + \omega^2\sin^2(\chi-\theta)) + I_3\omega^2\cos^2(\chi-\theta)] \\ & + \frac{1}{2}m\frac{g^2}{\omega^2}\left(\frac{\lambda}{L}\right)^2 \frac{\sin^2\theta}{1 - (\lambda/L)^2\sin^2\theta} \\ & - mg \cdot [L + (\lambda-\varepsilon)(1-\cos\theta) - \sqrt{L^2 - \lambda^2\cdot\sin^2\theta}] \end{aligned} \tag{B.10}$$

and the conjugated momentum of θ is

$$p_\theta = \frac{\partial L}{\partial\dot{\theta}} = \left[m(\lambda-\varepsilon)^2\sin^2\theta\left(1 + \frac{\lambda^2}{(\lambda-\varepsilon)}\frac{\cos\theta}{\sqrt{L^2 - \lambda^2\sin^2\theta}}\right)^2 + I_{12}\right]\cdot\dot{\theta}. \tag{B.11}$$

The Hamiltonian [1–4] of our system is

$$H = p_\theta\cdot\dot{\theta} - L = \frac{p_\theta^2}{2\big[m(\lambda-\varepsilon)^2\sin^2\theta\big(1 + \frac{\lambda^2}{(\lambda-\varepsilon)}\frac{\cos\theta}{\sqrt{L^2-\lambda^2\sin^2\theta}}\big)^2 + I_{12}\big]} + V_{\text{eff}}(\theta), \tag{B.12}$$

where $V_{\text{eff}}(\theta)$ is the effective potential given by

$$\begin{aligned} V_{\text{eff}}(\theta) = {} & -\frac{1}{2}\omega^2(I_{12}\sin^2(\chi-\theta) + I_3\cos^2(\chi-\theta)) - \frac{1}{2}m\frac{g^2}{\omega^2}\left(\frac{\lambda}{L}\right)^2\frac{\sin^2\theta}{1-(\lambda/L)^2\sin^2\theta} \\ & + mg\cdot(L + (\lambda-\varepsilon)(1-\cos\theta) - \sqrt{L^2 - \lambda^2\sin^2\theta}) \end{aligned} \tag{B.13}$$

and

$$\begin{aligned} \frac{\partial V_{\text{eff}}(\theta)}{\partial\theta} = {} & -\omega^2\sin\theta\cos\theta|I_{12} - I_3| + mg\sin\theta \\ & \cdot\left((\lambda-\varepsilon) + \frac{\lambda^2\cos\theta}{\sqrt{L^2-\lambda^2\sin^2\theta}} - \frac{g}{\omega^2}\left(\frac{\lambda}{L}\right)^2\frac{\cos\theta}{\big(1-(\lambda/L)^2\sin^2\theta\big)^2}\right). \end{aligned} \tag{B.14}$$

Therefore, to first-order expansion in the ratio (ε/L), $V_{\text{eff}}(\theta)$ has a minimum for $\theta = \theta_0 \neq 0$ when the following condition is satisfied:

$$\cos\theta_0 = +\frac{mg(\lambda-\varepsilon)}{|I_{12}-I_3|\omega^2}\cdot\left(1+\frac{\lambda^2\cos\theta_0}{(\lambda-\varepsilon)L}\left[\frac{1}{\sqrt{1-(\lambda/L)^2\sin^2\theta_0}}-\frac{(g/\omega^2L)}{(1-(\lambda/L)^2\sin^2\theta_0)^2}\right]\right) \quad \text{for} \quad \omega \geqslant \omega_{\text{crit}}. \tag{B.15}$$

This equation describes the relation between θ and ω, similar to equation (A.9) for the previous model. As in that case, the values of θ and ω can be found recursively. For $\omega = \omega_{\text{crit}}$, $\theta_0 = 0$ therefore

$$\omega_{\text{crit}}^2 = \frac{gm(\lambda-\varepsilon_c)}{|I_{12}-I_3|}\cdot\left[1+\frac{\lambda^2}{L(\lambda-\varepsilon_c)}-\frac{\varepsilon_c}{(\lambda-\varepsilon_c)}\frac{\lambda}{L}\right] = \frac{gm(\lambda-\varepsilon_c)}{|I_{12}-I_3|}\cdot\left[1+\frac{\lambda}{L}\right], \tag{B.16}$$

where according to (A.4) $\varepsilon_c = \varepsilon(\omega_{\text{crit}}, \theta = 0) = \left(g/\omega_{\text{crit}}^2\right)(\lambda/L)$.

As was discussed in section 2, the condition $\partial V_{\text{eff}}/\partial\theta = 0$ for $\omega < \omega_{\text{crit}}$ will be satisfied only for $\theta_0 = 0$.

For the case of a ring, with an external radius R_{ex} and an internal radius R_{in} we have that

$$2I_{12} \approx I_3 = m\left(\frac{R^2+R_{\text{ex}}^2}{2}\right) \qquad \text{and} \qquad \lambda-\varepsilon \approx R_{\text{ex}}, \tag{B.17}$$

therefore the relation between θ_0 and ω is according to (B.15), for $\omega \geqslant \omega_{\text{crit}}$ we have

$$\omega^2 \approx +\frac{4g}{R_{\text{ex}}\cos\theta_0}\cdot\frac{1}{(1+(R_{\text{in}}/R_{\text{ex}})^2)} \times\left(1+\frac{R_{\text{ex}}}{L}\left(1+\frac{2\varepsilon}{R_{\text{ex}}}\right)\frac{\cos\theta_0}{\sqrt{1-(R_{\text{ex}}/L)^2(1+\varepsilon/R_{\text{ex}})^2\sin^2\theta_0}}B\right), \tag{B.18}$$

with

$$B = 1-\frac{\varepsilon}{(R_{\text{ex}}+\varepsilon)}\frac{1}{(1-(R_{\text{ex}}/L)^2(1+\varepsilon/R_{\text{ex}})^2\sin^2\theta_0)}. \tag{B.19}$$

Neglecting the terms in $(\varepsilon/R_{\text{ex}})$, equation (B.18) can be approximated by

$$\omega^2 \approx +\frac{4g}{R_{\text{ex}}\cos\theta_0}\cdot\frac{1}{(1+(R_{\text{in}}/R_{\text{ex}})^2)}\left(1+\frac{R_{\text{ex}}\cos\theta_0}{\sqrt{L^2-R_{\text{ex}}^2\sin^2\theta_0}}\right) \qquad \text{for} \quad \omega \geqslant \omega_{\text{crit}}. \tag{B.20}$$

In the case of the hollow bar of length h and diameter d, that is attached to a wire at a distance δ from its extreme, we have

$$I_{12} = \tfrac{1}{12}mh^2, \qquad \text{and} \qquad I_3 = \tfrac{1}{4}md^2 \tag{B.21}$$

consequently from expression (B.16) we have

$$\omega_{\text{crit}}^2 = \frac{6g}{h}\cdot\frac{(1-2\delta/h)}{(1-3(d/h)^2)}\left(1+\frac{h}{2L}+\frac{(\varepsilon_c-\delta)}{L}\right), \tag{B.22}$$

and

$$\omega_{\text{crit}}^2 = \frac{6g}{h}\cdot\left(1-\frac{2\delta}{h}\right)\left[1+\frac{h}{2L}+\frac{\varepsilon_c-\delta}{L}\right] \approx \omega_{c0}^2\left(1+\frac{h}{2L}-\frac{2\delta}{h}+\frac{\varepsilon_c-\delta}{L}\right). \tag{B.23}$$

This last approximation is valid for the usual case when $d \ll h$, ε_c and $\delta \ll h$ and $h < L$. Expression (B.23) indicates very clearly the effect of the finite length of the wire and the distance δ on ω_{crit}. Figure 6 illustrates these effects on the value of ω_{crit}. Figure 9 shows the shape of the effective potential for two different angular velocities, one for $\omega < \omega_{\text{crit}}$ and

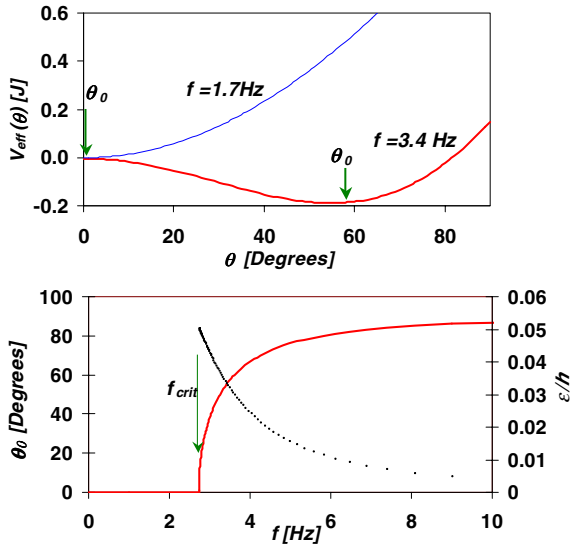

Figure 9. Top: shows the effective potential as a function of the angle for two different frequencies, one below and another above the critical frequency ($f_{\rm crit} = 2.8$ Hz, for a bar of length $h = 25.5$ cm). In the first case the minimum occurs for $\theta_0 = 0$ and in the second case at about $\theta_0 = 55^\circ$. Bottom: the variation of the equilibrium angle θ_0 as a function of the rotating frequency as described by equation (B.15), referred to the left vertical axis. The dotted line represents the variation of the ratio ε/h as a function of the frequency, calculated using the recursive procedure described in the text.

another for $\omega > \omega_{\rm crit}$, for the rod of length $h = 25.5$ cm. The lower panel of this figure shows the variation of θ_0 with the rotational frequency f for the case of a bar as predicted by equation (B.15). The lower panel also shows the ratio of ε/h as a function of f, referred to the right vertical axis.

The effective potential for the naïve model can also be obtained introducing

$$I_3 \approx 0, \qquad I_{12} = \frac{1}{12} m \cdot h^2, \qquad \lambda - \varepsilon = h/2 \qquad \text{and} \qquad \frac{\lambda}{L} \approx \frac{h}{2L} \to 0; \tag{B.24}$$

into equation (B.13), i.e.,

$$V_{\rm eff}(\theta) = mg\frac{h}{2}(1 - \cos\theta) - \frac{1}{2}\omega^2 I_{12} \sin^2\theta. \tag{B.25}$$

Here $I_{12} \sin^2\theta$ is the moment of inertia of the inclined rod. This expression indicates that, in the space-fixed frame, the effective potential has two terms, the gravitational potential and the centrifugal potential (second term on the right-hand side), that tend to bring the bar to a horizontal position. It is interesting to note that the total energy of this system, for a constant value of θ, would also contain the same terms as equation (B.25). However, in this case both components of the total energy have a positive sign, making it difficult to explain the behaviour of this system and giving rise to the apparent paradox.

If we take the derivative of the effective potential with respect to θ, we obtain the net torque on the rod in the space-fixed frame of reference

$$\tau_{\rm eff} = -\frac{\partial V_{\rm eff}(\theta)}{\partial\theta} = -mg\frac{h}{2}\sin\theta + \omega^2 I_{12}\sin\theta\cos\theta. \tag{B.26}$$

The first term on the right-hand side is the torque due to the vertical component of string tension (here the torque due to the horizontal component is negligible because $L \gg h$). The second term is the component of the torque that tends to bring the bar to a horizontal position. This last term is strongly dependent on the frequency of rotation and it cancels at $\theta = 0^\circ$ and $\theta = 90^\circ$. In the space-fixed frame its physical origin is a consequence of Newton's first law or principle of inertia. At low frequencies the only stable position of the bar occurs at $\theta = 0^\circ$, see figure 9. At higher frequencies the equilibrium between these two torques moves to larger angles as indicated in figure 9, in agreement with our heuristic argument carried out in the rotating system of reference, presented in the introduction to justify the naïve model.

References

[1] Goldstein H, Poole C and Safko J 2001 *Classical Mechanics* 3rd edn (Reading, MA: Addison-Wesley)
[2] Marion J B 1970 *Classical Dynamics* 2nd edn (New York: Academic)
[3] Sommerfeld A 1964 *Mechanics* (New York: Academic)
[4] McCuskey S W 1959 *An Introduction to Advanced Dynamics* (Reading, MA: Addison-Wesley)
[5] Amengual A 1996 On a simple experiment on the free rotation of a ruler and other laminas *Am. J. Phys.* **64** 82–7
[6] Rueckner W, Georgi J, Goodale D, Rosenberg D and Tavilla D 1995 Rotating saddle Paul trap *Am. J. Phys.* **63** 186–7
[7] Kalotas T M and Lee A R 1990 A simple device to illustrate angular momentum conservation and instability *Am. J. Phys.* **58** 80
[8] Daw H A and Daw Pomeroy M R 2001 The free rotator apparatus *Am. J. Phys.* **69** 389–93
[9] Moisy F 2003 Supercritical bifurcation of a spinning hoop *Am. J. Phys.* **71** 999–1004